Naval Research Laboratory
Washington, DC 20375-5320

NRL/7220/MR—2022/4

Estimating the Net Radiative Impact of Stratospheric Pyrocumulonimbus Plumes

GEORGE P. KABLICK III

Middle Atmosphere Physics Section
Remote Sensing Division

November 4, 2022

REPORT DOCUMENTATION PAGE

Form Approved
OMB No. 0704-0188

1. REPORT DATE *(DD-MM-YYYY)*	**2. REPORT TYPE**	**3. DATES COVERED** *(From - To)*
04-11-2022	NRL Memorandum Report	11-23-2019 – 11-23-2021

4. TITLE AND SUBTITLE

Estimating the Net Radiative Impact of Stratospheric Pyrocumulonimbus Plumes

5a. CONTRACT NUMBER

5b. GRANT NUMBER

5c. PROGRAM ELEMENT NUMBER
NISE

6. AUTHOR(S)

George P. Kablick III

5d. PROJECT NUMBER

5e. TASK NUMBER

5f. WORK UNIT NUMBER
N2V9

7. PERFORMING ORGANIZATION NAME(S) AND ADDRESS(ES)

Naval Research Laboratory
4555 Overlook Avenue, SW
Washington, DC 20375-5320

8. PERFORMING ORGANIZATION REPORT NUMBER

NRL/7220/MR--2022/4

9. SPONSORING / MONITORING AGENCY NAME(S) AND ADDRESS(ES)

Naval Research Laboratory
4555 Overlook Avenue, SW
Washington, DC 20375-5320

10. SPONSOR / MONITOR'S ACRONYM(S)

NRL/NISE

11. SPONSOR / MONITOR'S REPORT NUMBER(S)

12. DISTRIBUTION / AVAILABILITY STATEMENT

DISTRIBUTION STATEMENT A: Approved for public release; distribution is unlimited.

13. SUPPLEMENTARY NOTES

Karles Fellowship

14. ABSTRACT

Estimates of the global radiative impact of stratospheric plumes are continually being refined as improvements are made to measurements and the source become better understood. One such source that has long been overlooked are pyrocumulomibus storms. Plumes from these events range from short-lived, localized injections of smoke aerosols above the tropopause to the more extreme hemisphere-covering plumes that can last on seasonal timescales. In addition to the aerosol component, water vapor is present in many of these plumes in radiatively significant amounts. However, the boundary fluxes of this strong radiative forcing species have never been explored in the context of pyrocumulonimbus plumes. In this project a case study demonstrates that the downwelling flux at the surface is increased by up to 0.3 W/m2, and an upwelling flux at the top-of-atmosphere is decreased by 0.01 W/m2. The net effect of this forcing is a longwave heating of 0.05 K/day within the stratospheric plume.

A significant discovery was made during this project that directly resulted from the heating present within these pyrocumulonimbus plumes. This discovery was unanticipated, but shows that the net heating within these plumes effect the dynamics of the statosphere. A dynamical anomaly characterized by a rotating spheroid of smoke aerosols and biomass burning gases is generated as the plume absorbs radiation and generates buoyancy through diabatic heating. This phenomenon has been termed Smoke With Induced Rotation and Lofting (SWIRL), and is shown in this report to be associated with much longer plume lifetimes and synoptic-scale weather anomalies that were unknown prior to this study. The effect of this discovery has led to a new vein of research within stratospheric dynamic models, and has successfully formed the basis of a 6.1 New Start proposal. The case study which allowed for the discovery of this phenomenon is introduced in this report, and the details of the dynamical impact and the increased lifetime are compared with previous cases.

15. SUBJECT TERMS

Pyrocumulonimbus
Radiative transfer
Stratosphere
Dynamics

16. SECURITY CLASSIFICATION OF:			**17. LIMITATION OF ABSTRACT**	**18. NUMBER OF PAGES**	**19a. NAME OF RESPONSIBLE PERSON**
					George P. Kablick III
a. REPORT	**b. ABSTRACT**	**c. THIS PAGE**	U	14	**19b. TELEPHONE NUMBER** *(include area code)*
U	U	U			(202) 767-2904

Standard Form 298 (Rev. 8-98)
Prescribed by ANSI Std. Z39.18

This page intentionally left blank.

Executive Summary

This report presents research conducted by George Kablick under the Karles Fellowship for the period of 23 November 2019 through 23 November 2021. This work focuses on calculating radiative transfer estimates through pyrocumulonimbus (pyroCb) plumes using a case study approach with offline models (see References for published work cited in this report). In the final year of the fellowship, the fellow focused some of his efforts towards preliminary studies for a newly funded 6.1 New Start for which he is a Co-I: "PyroCb-Generated SWIRLs in the Stratosphere."

Estimates of the global radiative impact of stratospheric plumes are continually being refined as improvements are made to measurements and the source become better understood. One such source that has long been overlooked are pyroCb storms. Plumes from these events range from short-lived, localized injections of smoke aerosols above the tropopause to the more extreme hemisphere-covering plumes that can last on seasonal timescales. In addition to the aerosol component, water vapor is present in many of these plumes in radiatively significant amounts. However, the boundary fluxes of this strong radiative forcing species have never been explored in the context of pyroCb plumes. In this project a case study demonstrates that the downwelling flux at the surface is increased by up to 0.3 W m^{-2}, and an upwelling flux at the top-of-atmosphere is decreased by 0.01 W m^{-2}. The net effect of this forcing is a longwave heating of 0.05 K/day within the stratospheric plume.

A significant discovery was made during this project that directly resulted from the heating present within these pyroCb plumes. This discovery was unanticipated, but shows that the net heating within these plumes effect the dynamics of the stratosphere. A dynamical anomaly characterized by a rotating spheroid of smoke aerosols and biomass burning gases is generated as the plume absorbs radiation and generates buoyancy through diabatic heating. This phenomenon has been termed Smoke With Induced Rotation and Lofting (SWIRL), and is shown in this report to be associated with much longer plume lifetimes and synoptic-scale weather anomalies that were unknown prior to this study. The effect of this discovery has led to a new vein of research within stratospheric dynamic models, and has successfully formed the basis of the aforementioned 6.1 New Start proposal. The case study which allowed for the discovery of this phenomenon is introduced in this report, and the details of the dynamical impact and the increased lifetime are compared with previous cases.

This page intentionally left blank.

Estimating the Net Radiative Impact of Stratospheric Pyrocumulonimbus Plumes

Karles Fellow: George P. Kablick III

Project Objective

The goals of this project were to estimate the radiative and dynamical signatures of several noteworthy pyrocumulonimbus (pyroCb) plumes in the upper troposphere/lower stratosphere (UTLS) using satellite remote sensing datasets, radiative transfer models, and global reanalysis.

Motivation

Stratospheric injection of clouds and tropospheric air from thunderstorm convection is relatively uncommon [*Holton et al.*, 1995]. The vertically-towering convective clouds that are typical of meteorological thunderstorms are called cumulonimbus (Cb). These events are characterized by an unstable atmosphere and a "trigger" that initiates convection, such as a dynamical perturbation to the air column, or a diabatic source such as solar heating of the surface. A small subset of convective thunderstorms are triggered from the heat of wildfires. These events are called pyroCbs, and only constitute a small fraction of convection that occurs every year globally (approximately 40 events/year) [*Fromm et al.*, 2010]. However these pyroCbs, despite their relative infrequency, are very intense. The strength of their convection frequently causes an overshoot of the tropopause, where they pollute the stratosphere with plumes consisting of carbonaceous aerosol mixtures and trace gases such as water vapor and carbon monoxide. Several recent pyroCb events and publications have shown that these plumes can persist for months, covering horizontal distances on the scale of an entire hemisphere, and rising from the tropopause to well into the middle stratosphere bringing along with them the biomass burning species that are not normally present in great abundance. Therefore, there is a strong need to analyze pyroCb plumes in the context of several observable effects to understand the full potential that these events could have on climate forcing. These effects include localized phenomena, such as their unique remote sensing signatures like lidar depolarization ratio and radar frequency sensitivity, and they include broader effects such as their observable stratospheric lifetime, and dynamical anomalies caused by solar heating of the dark aerosols. With these needs in mind, the objectives of this project were to analyze the radiative transfer and dynamics of pyroCb plumes in the UTLS.

Technical Approach and Progress

The approach of this project was to quantify the amount of several signature features of pyroCb plumes including aerosol concentration, and mixing ratios of water vapor and

Manuscript approved November 3, 2022.

carbon monoxide. With the aid of models, satellite observations of these variables were used to understand how they influence the dynamics and stratospheric advection of the plumes. The focused analysis was on three well-published case studies referred to as the Great Slave Lake (GSL) pyroCb from 5 August 2014 [*Kablick et al.*, 2018], Pacific Northwest pyroCb Event (PNE) from 12 August 2017 [*Peterson et al.*, 2018], and the Australian New Year pyroCb Event (ANY) from 31 December 2019–4 January 2020 [*Kablick et al.*, 2020; *Allen et al.*, 2020]. This project relied on several remote sensing instrument datasets, a radiative transfer model, and a general circulation model to understand these effects.

Observational Datasets

The suite of Earth Observing System NASA satellite instruments flying in a formation called the "A-Train" was designed to take advantage of observations made by several instruments with different sensitivities at the same geolocation. The main instruments used in this study from the A-Train include the Microwave Limb Sounder (MLS) and Cloud-Aerosol LIdar with Orthogonal Polarisation (CALIOP). MLS is a passive microwave profiling instrument that retrieves many chemical species in the upper atmosphere on pressure surfaces. It also retrieves temperature and geopotential height profiles. CALIOP is a frequency-doubled lidar with visible (532 nm) and near-infrared (1064 nm) channels with depolarization at 532 nm. For the period of study contained herein, both MLS and CALIOP observations were spatiotemporally colocated, allowing for an analysis of contemporaneous aerosols, hydrometeors and trace gases produced by pyroCbs.

Models

The models used in this study include two offline radiative transfer models (RTMs) with different capabilities, and the Navy Global Environmental Model (NAVGEM) reanalysis. The two RTMs include the Line-By-Line Radiative Transfer Model (LBLRTM) [*Clough et al.*, 1992] and the Santa Barbara DISORT Radiative Transfer model (SBDART) [*Ricchiazzi et al.*, 1998]. The LBLRTM framework is used to estimate longwave water vapor forcing associated with pyroCb plumes. This model uses the extremely detailed HITRAN 2016 database of line spectra for H_2O and about 50 additional trace species [*Gordon et al.*, 2017]. However, it is computationally inefficient to compute band-averaged fluxes using LBLRTM when complex aerosol or cloud layers are present, so the pyroCb aerosol profiles are computed by the plane-parallel model SBDART.

As a primer, it is useful to illustrate the sensitivity of fluxes to changes in water vapor. This is shown through a comparison of radiative fluxes in an an idealized atmosphere with those in an atmosphere with small water vapor perturbations. For example, small changes in column water vapor mixing ratio (WVMR) in the stratosphere can lead to climate-significant radiative forcing (RF) via changes in fluxes and heating rates. When climate feedbacks and chemistry changes are ignored, this is referred to as an instantaneous RF, and represents a starting estimate of the net forcing (the forcing produced by parameterized climate models). Instantaneous RF is defined in terms of the upward and downward flux ($F^{\uparrow}$

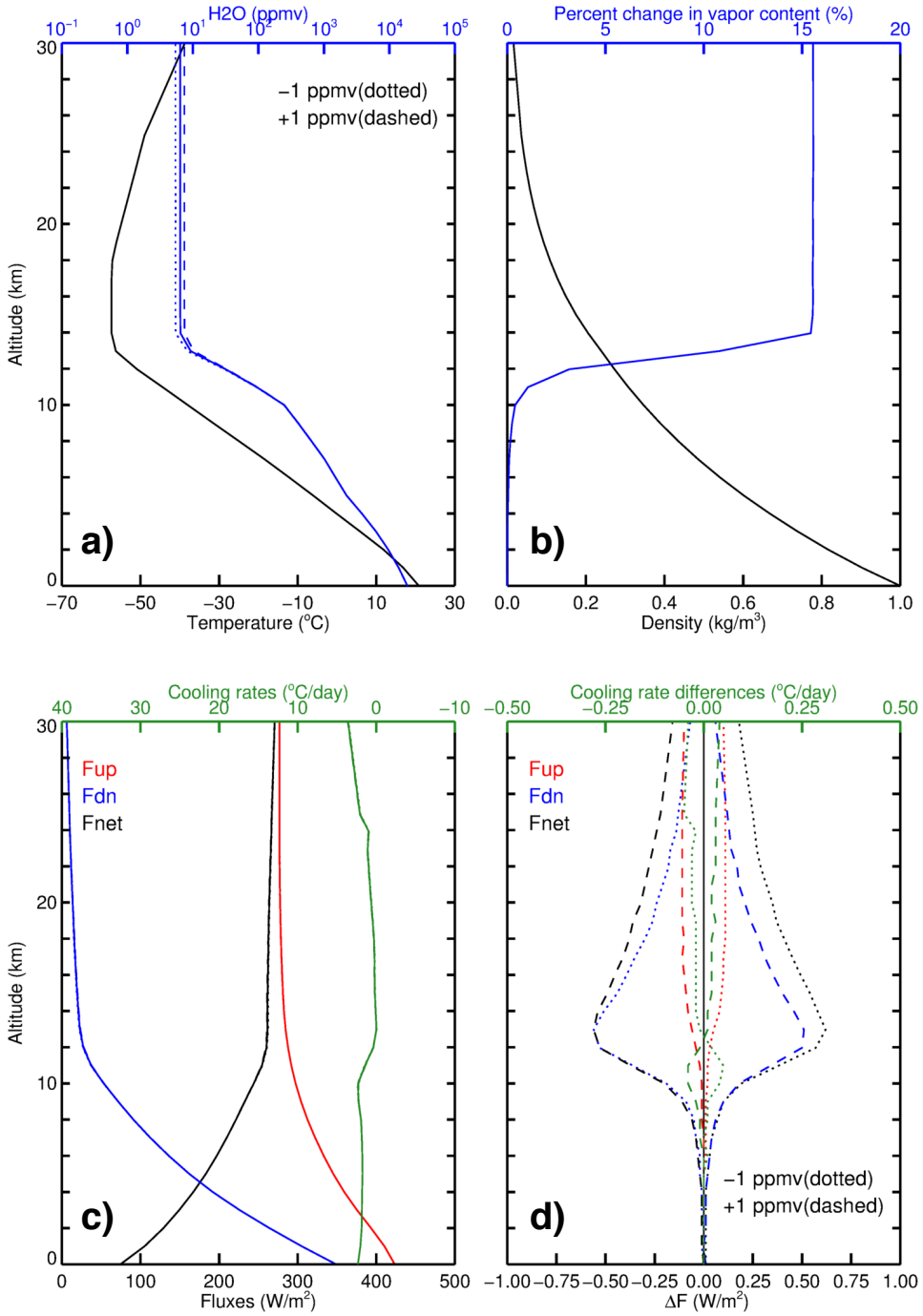

Figure 1: Perturbations and radiative transfer through AFGL midlatitude atmosphere. Model profiles in each panel show (a) temperature (black) and WVMR (blue), where the solid line is the standard mixing ratio and dashed/dotted lines are the +1 or −1 ppmv perturbations; (b) air density (black) and the percentage WVMR perturbation (blue); and (c) longwave fluxes (upward; red, downward; blue, net; black) and cooling rates (green). The eight lines in (d) are the flux and cooling rate differences between the +1 or −1 ppmv perturbations on the standard model results shown in (c).

and $F^{\downarrow}$, respectively) as the inverse of the change in net flux (F^{net}) from a control state:

$$RF = -\Delta F^{net}, \tag{1}$$

where

$$\Delta F^{net} = (F^{\uparrow} - F^{\downarrow})_{anomaly} - (F^{\uparrow} - F^{\downarrow})_{control}. \tag{2}$$

Figure 1 shows the forcing experienced by imposing a ±1 ppmv water vapor anomaly on the Air Force Geophysical Laboratory (AFGL) standard midlatitude atmosphere ("control"). This figure shows the WVMR change in terms of an absolute amount (a) and an altitude-relative percentage (b). Temperature (a) and air density profiles (b) are held constant, and the radiative flux and cooling rate for both the control and the perturbed WVMR profiles are shown. Changes in WVMR are most influential in the longwave part of the electromagnetic spectrum (wavenumber between 10–3000 cm^{-1}), so that is the focus here. This figure shows that increasing WVMR throughout the column increases $F^{\downarrow}$ at the tropopause while slightly decreasing $F^{\uparrow}$ (blue and red dashed lines in Figure 1d, respectively). The black dashed line is ΔF^{net}, which shows that the effect of increasing column WVMR by 1 ppmv is to create a positive longwave RF. Keeping with convention for longwave radiative transfer, the cooling rate is defined as the flux divergence in a layer ($-\nabla \cdot F^{net}$). In other words, if a volume of air has more radiative energy leaving it than coming into it, there will be a "positive cooling." The opposite is also true: positive differential of net flux (more energy in than out) results in a "negative cooling" (i.e., warming). In this case, when comparing an atmosphere with an increase in WVMR to the control atmosphere, a negative cooling rate difference indicates warming with respect to the control (Figure 1d). This simple example illustrates the importance of understanding changes in stratospheric H_2O in the context of RF.

Putting this into context with an example from the relatively small GSL pyroCb plume (Figure 2), it is apparent that a >1 ppmv increase of UTLS water vapor is possible from a pyroCb plume, and not just from direct entrainment of moist tropospheric air, but from the sublimation of ice present in the plume/cloud mixture. In this figure, the GSL plume is tracked for approximately 2 weeks post-injection and MLS ice water content (IWC) closely follows an independent estimation of ice (CALIOP depolarization ratio: δ_{532}). As these two proxies for ice decrease, MLS water vapor mixing ratio increases, adding confirmation to the hypothesis that ice injected in pyroCb plumes can locally hydrate the UTLS, and subsequently impact its radiative energy budget. This example focuses on WVMR only, wereas it is important to consider aerosols and ice as well because they are also active absorbers. Future work will account for these variables, but the focus of the present Report is on WVMR. In a later section an initial estimate of aerosol heating will be discussed.

Results

In 2017 the PNE pyroCb case set a new benchmark for stratospheric water vapor intrusion from a pyroCb plume. The largest plume from this event could be tracked for about three months using MLS WVMR observations. Anomalies of WVMR are shown in Figure 3a based on a Lagrangian technique used to track the plume and find relevant satellite intersections (red shaded contours). These anomalies were created by first constructing a spatiotemporal stratospheric climatology of all 2006–2017 MLS H_2O observations (dark gray contours), and

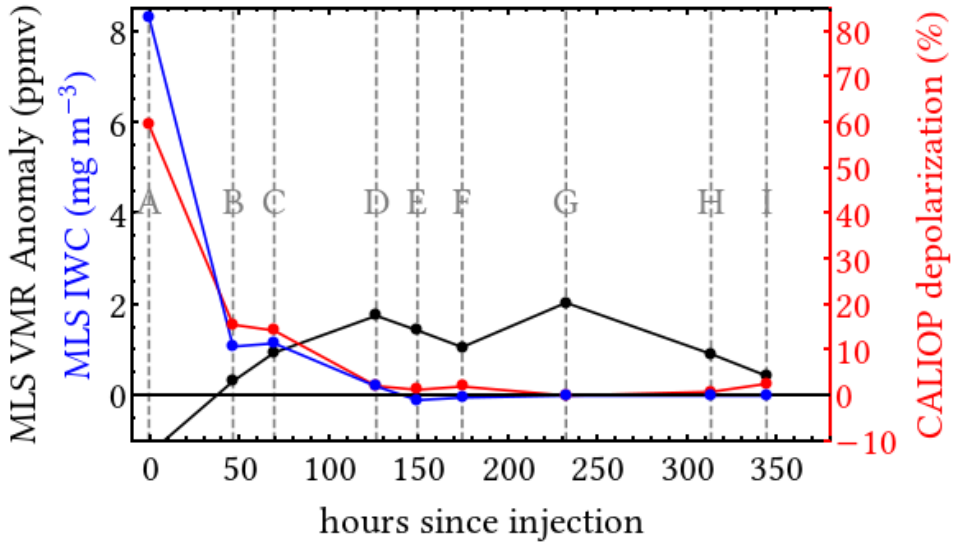

Figure 2: Mean values of MLS WVMR anomalies and IWC (black and blue lines, respectively) and median CALIOP δ_{532} (red line) over the two-week observable lifetime of the GSL pyroCb plume. Each MLS point in this time series represents a per-profile vertical mean between 360–400 K for measurements encompassing the plume (vertical dashed lines indicate time since injection), and each CALIOP point is the median value for the entire "stratospheric feature" between 360–400 K. [*Kablick et al.*, 2018]

subtracting it from the individual profile observations through the plume. The specific details of the climatology are: i) it is zonally-averaged for both the tropical (30 °S to 30 °N) and mid-latitude (30 °N to 60 °N) bands, and ii) the troposphere temperature, pressure and humidity profiles are held constant using the AFGL Tropical (TRP), MidLatitude Summer (MidLatS) and MidLatitude Winter (MidLatW) standard soundings. The TRP sounding is applied during the entire year in the 30 °S to 30 °N band, but for 30 °N to 60 °N the MidLatS is applied between August–October, and the MidLatW is applied between November–March. The stratospheric component to this climatology is date-specific, according to the value determined by averaging the MLS record on that date for that latitude band for every year during 2006–2017. Light gray vertical bars show dates when MLS did not observe the plumes.

The WVMR climatology shows typical values $\sim$ 4–5 ppmv within the altitude of the plume at $20 < z < 25$ km (Figure 3a). This plume has anomalies > 7 ppmv in the early days of this time series, and as it ages, the anomalies reduce to values between 2–3 ppmv. Figure 3b shows the corresponding longwave heating anomalies (ΔQ_{LW}) from LBLRTM. The model is run for both the MLS observation profile (with Fixed Anomaly vertical constraints) and the climatology profile, and then differenced to determine ΔQ_{LW}. There is a cooling enhancement within the plume down to -0.5 K day^{-1} during the early days, and a very small warming enhancement throughout the depth of the troposphere of $< +0.05$ K day^{-1}. There is cooling within and above the upper section of WVMR plume anomaly because it of its enhanced absorption and re-emission at colder temperatures of terrestrial longwave radiation from below. Results from this plume recreate the classic positive *RF* scenario discussed in

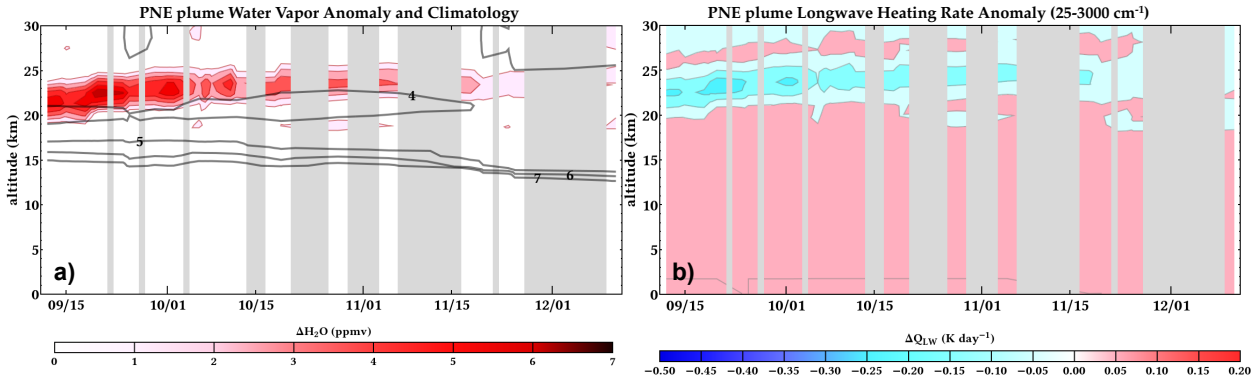

Figure 3: (a) Aura MLS WVMR anomalies and climatologies (black contours) within the main 2017 PNE pyroCb plume after 12 September. All contours in ppmv. (b) Longwave LBLRTM heating rate anomalies throughout the troposphere and lower stratosphere computed from these observations. Vertical gray bars indicate where MLS missed observations.

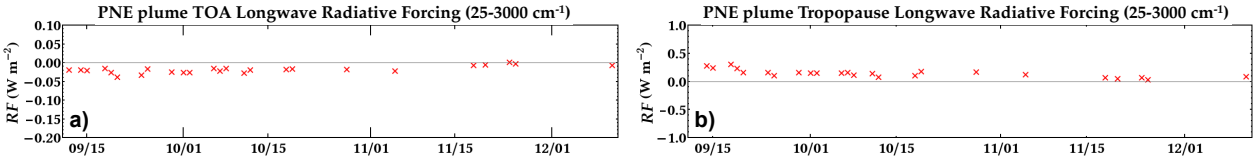

Figure 4: (a) TOA and (b) tropopause-level longwave *RF* using the MLS WVMR anomalies from Figure 3. This plume is confined to the tropics for most of its observable duration, and has a negative *RF* at TOA (a decrease in OLR), and there is a positive *RF* at the tropopause.

introductory radiative transfer texts used to illustrate first-order global warming.

An interesting discovery made during this case is the upward motion of the plume as it ages. This upward motion has since been attributed to the buoyancy created from the diabatic warming by solar absorption of the smoke aerosols. Prior to this 2017 case, it was not thought that pyroCb plumes could become buoyant in the stable layers of the stratosphere. In the largest of the case studies included in this project, the 2019-20 ANY Event, it was also discovered that this buoyant uplift resulted in a dynamical perturbation to the wind field. The result was a rotating, uplifting smoke plume that was named Smoke With Induced Rotation and Lofting (SWIRL) [*Allen et al.*, 2020].

Discovery of the SWIRL

In the initial stages of studying the ANY Event, it was noticed that it had produced an unprecedented intrusion of H_2O into the stratosphere. Until this event, Aura MLS had not reported WVMR >15 ppmv at any of its pressure retrieval levels between 39-12 hPa except for an apparent measurement anomaly in 2012. However, on 20 January 2020, MLS observed H_2O to have values >15 ppmv at a pressure of 38.3 hPa, and in the month to follow (February 2020) there were 59 MLS observations of H_2O>15 ppmv at 17.8 hPa, and four at 12.1 hPa.

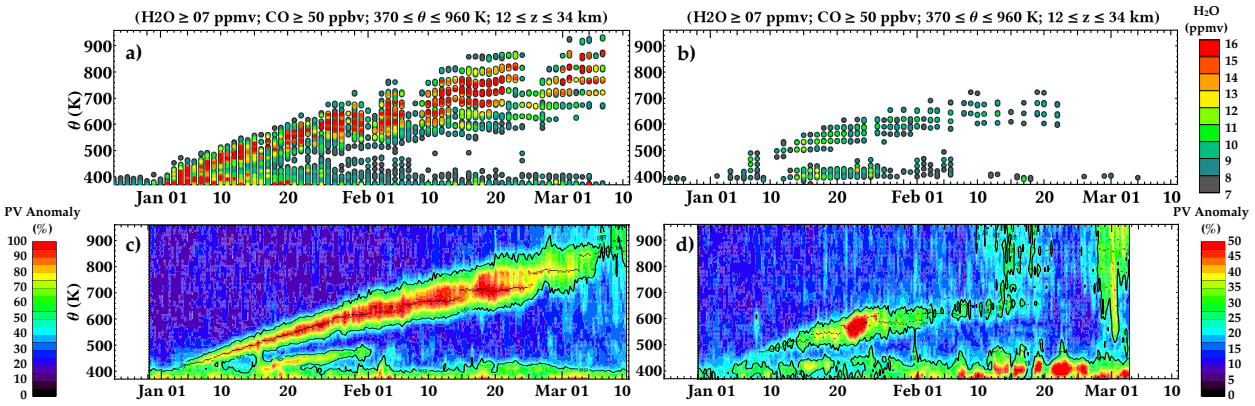

Figure 5: (a) θ at MLS profile maximum H_2O of the ANY Event SWIRLs. Red dots indicate H_2O>15 ppmv (maximum value ∼23 ppmv in mid-January). P1 contributes the bulk of these observations. (b) Same as a) but only locations corresponding to P2. (c) The maximum PV anomaly from NAVGEM analysis. P1 is the top-most ascending branch of PV. Black contour: 50% isoline; black dots: θ-midpoint of P1. (d) Same as (c) but only locations corresponding to P2. Black contour: 25% isoline. Note color scale difference between (c) and (d).

Figure 5a shows the transport of this stratospheric WVMR intrusion on a coordinate grid of potential temperature (θ), which is a standard way to display vertically-resolved stratospheric variables. Shown are the maximum WVMR per MLS profile between 15° N and 90° S that match certain threshold criteria: 1) volume mixing ratios of H_2O and CO must be >7 ppmv and >50 ppbv, respectively, and 2) geopotential height and θ must be between 12-34 km and 370-960 K, respectively. This methodology limits false-positives (e.g., tropical overshooting convection), and helps track LS smoke in the earliest days of the largest SWIRL (called P1). Figure 5b uses the same methodology, but isolates the latitude and longitude to identify a secondary, smaller SWIRL (called P2) that formed from the same event. In both instances the diabatic rise of the plume containing this H_2O/CO is the prominent feature.

This result was published soon after the ANY Event occurred, and introduced the idea that pyroCb plumes, through the SWIRL phenomenon, can as "containment vessels" for the upward propagation of aerosols and lower stratospheric air because of their long-lived and stable rotation as they move upward [*Kablick et al.*, 2020]. Figure 6a shows a cross section of the P1 SWIRL from the ANY Event. The shaded red and blue contours represent Ertel potential vorticity (PV) anomalies computed from NAVGEM, and is a dynamical variable representing the rotation of air. These anomalies are expressed as a percent relative to the surrounding air at similar latitudes, so the red contours show the location of strong rotation. Overlaid on top of this PV anomaly are contours of winds: black solid and dashed contours represent northward and southward winds, respectively; and temperature anomalies: blue solid and dashed contours represent positive and negative temperature anomalies, respectively. The result is a rotation rate of approximately 15 m s^{-1}. Using NAVGEM reanalysis revealed a temperature anomaly dipole structure, which presumably was due to the differential rates of absorption by the aerosols, and the dynamical response due to rotation. Figure 6b is a plan view of this large P1 SWIRL, and an additional smaller SWIRL, called P2 is visible over Antarctica. An introduction to this SWIRL phenomenon was presented in *Kablick et al.*

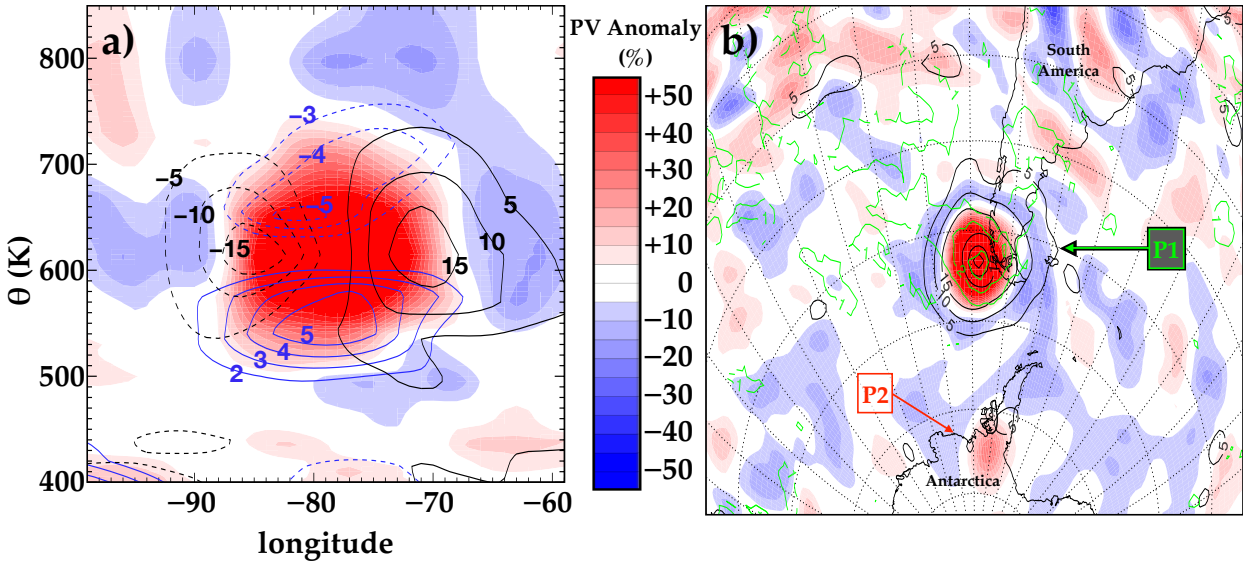

Figure 6: (a) Vertical cross section through P1 on 01/31, showing anticylonic rotation (black contours: m s^{-1}; solid: northward, dashed: southward), T-anomaly dipole (blue contours: °C), and PV anomaly (filled contours: %). (b) OMPS UVAI (green contours) shown with NAVGEM isotachs (black contours) and PV anomalies on 01/31 at θ=615 K. Peak windspeed ∼20 m s^{-1} and UVAI=3 near the center of the P1 PV anomaly. P2 anticyclone is weaker, but is dominant feature south of 60° S.

[2020], and a full dynamical description using NAVGEM was published in *Allen et al.* [2020].

One feature of SWIRLs has opened a new area of model improvement research into how to correct forecast errors. These errors occur from a lack of stratospheric aerosol physics in NAVGEM. Figure 7 shows two rows of images of the ANY P1 SWIRL, where the top row shows analysis fields of PV starting on 10 January 2020 and progressing in 2-day increments, and the bottom row shows forecast fields for the same dates. The analysis images are model PV fields that have gone through data assimilation. In other words, they take into account all relevant observations at each date, including stratospheric temperature profiles, to output meteorological fields. The bottom row, however, shows a series of forecasted model PV fields that only include observations at the initialization on 10 January. As the forecast is run, the PV anomaly from the SWIRL diminishes as NAVGEM doesn't account for the temperature perturbations of the aerosol layer.

There are two considerations that arise from this result. First, with the apparent increase in large pyroCb events over the past two decades, and with the likelihood that wildfires may become more widespread under current climate change projections, it is possible that these events will occur more frequently. Second, the datasets that are used by NAVGEM to initialize the model fields will change as certain instruments become decommissioned in the near future–the Aura satellite that hosts the MLS instrument is a prominent example. With these considerations, it is important to resolve the issues with these forecasts by improving the model physics.

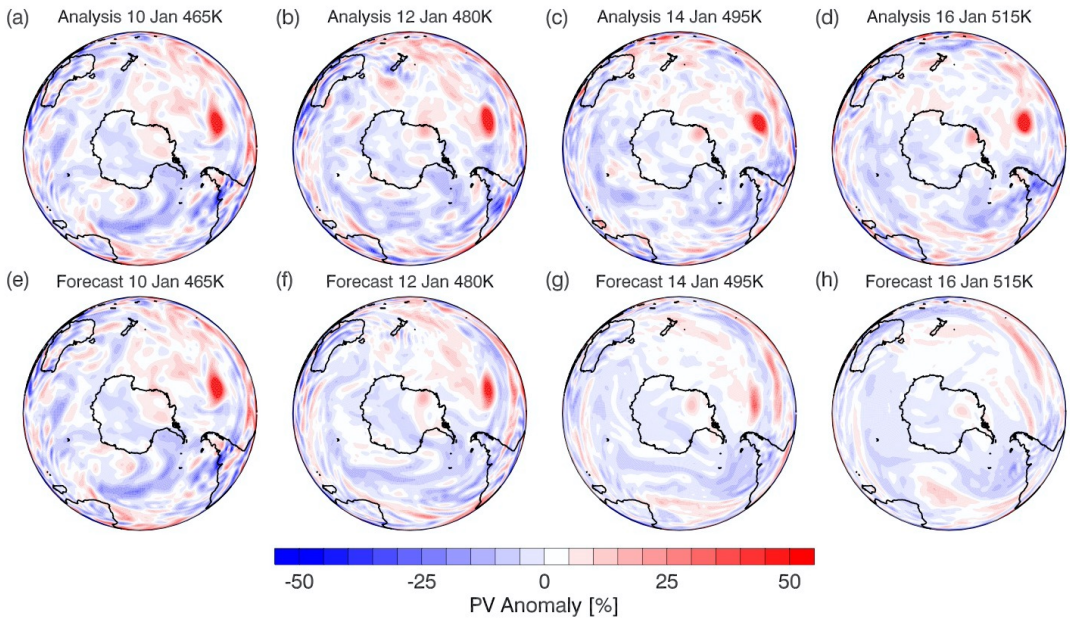

Figure 7: Southern Hemisphere potential vorticity anomaly (the percent difference from the zonal mean) from NAVGEM for 0000 UTC analyses steps on 10, 12, 14, and 16 January 2020 (top row) compared with the forecast anomaly at the same times initialized on 10 January 2020 at 0000 UTC (bottom row). The concentrated positive PV anomaly (red) in the southern Pacific Ocean is the SWIRL. Note its disappearance over time in the forecast as it persists in the analyses.

Plans

There is more work to be done to improve estimates of radiative effects, both in terms of individual plumes and the cumulative effects of a particular pyroCb season. The main objective of this project was to estimate the net effects using offline radiative transfer models, and while many goals were accomplished, the real-world net radiative influence of pyroCb plumes will rely on an expanded methodology. The results here provide some evidence that pyroCb plumes could have a climate-relevant influence on radiative energy budgets. Future work will involve a more thorough estimate of the RF while considering feedbacks in the model framework. This will require future development of NAVGEM capability to handle the physics of aerosol and the maintenance of SWIRL dynamics.

Many of the project's original objectives have been met, including estimating radiative impacts of stratospheric H_2O injected by select pyroCb events. There are several new questions that arose from this research project, including the frequency and magnitude of pyroCbs water vapor injections, and how SWIRLs act as dynamical barriers of upper tropospheric air as they propagate upward. The results presented herein provided the basis for a 3-year 6.1 New Start project that will begin in FY23. The goals of the New Start are to extend this analysis to additional cases by looking back through the historical record of pyroCb and identifying SWIRL events that were not noticed. Several high-profile cases have been identified recently that went unnoticed at the time they occurred, and there is strong

potential to improve our understanding of SWIRLs and NAVGEM's capability to handle them.

References

Allen, D., M. Fromm, G. Kablick, and G. Nedoluha (2020), Smoke with induced rotation and lofting (SWIRL) in the stratosphere, *Journal of the Atmospheric Sciences*, *77*(12), 4297–4316, doi:https://doi.org/10.1175/JAS-D-20-0131.1.

Clough, S., M. Iacono, and J. Moncet (1992), Line-by-Line Calculation of Atmospheric Fluxes and Cooling Rates: Application to Water Vapor, *J. Geophys. Res.*, *97*(D14), 15,761–15,785.

Dessler, A., M. Schoeberl, T. Wang, S. Davis, and K. Rosenlof (2013), Stratospheric water vapor feedback, *P. Natl. Acad. Sci. USA*, *110*(45), 18,087–18,091, doi:10.1073/pnas.1310344110.

Fromm, M., D. T. Lindsey, R. Servranckx, G. Yue, T. Trickl, R. Sica, P. Doucet, S. Godin-Beekmann, et al. (2010), The untold story of pyrocumulonimbus, *B. Am. Meteorol. Soc.*, *91*(9), 1193, doi:10.1175/2010BAMS3004.1.

Fromm, M., G. Kablick, D. Peterson, R. Kahn, V. Flower, and C. Seftor (2021), Quantifying the source term and uniqueness of the August 12, 2017 Pacific Northwest pyroCb event, *Journal of Geophysical Research: Atmospheres*, *126*(13), e2021JD034,928, doi:https://doi.org/10.1029/2021JD034928.

Gordon, I., L. Rothman, C. Hill, R. Kochanov, Y. Tan, P. Bernath, M. Birk, V. Boudon, A. Campargue, K. Chance, et al. (2017), The HITRAN2016 molecular spectroscopic database, *J. Quant. Spectrosc. Ra.*, *203*, 3–69.

Holton, J., P. H. Haynes, M. E. McIntyre, A. Douglass, R. Rood, and Pf. (1995), Stratosphere-troposphere exchange, *Rev. Geophys.*, *33*(4), 403–439, doi:10.1029/95RG02097.

Kablick, G., M. Fromm, S. Miller, P. Partain, D. Peterson, S. Lee, Y. Zhang, A. Lambert, and Z. Li (2018), The Great Slave Lake pyroCb of 5 August 2014: observations, simulations, comparisons with regular convection, and impact on UTLS water vapor, *J. Geophys. Res.*, *123*(21), 12–332, doi:10.1029/2018JD028965.

Kablick, G., D. Allen, M. Fromm, and G. Nedoluha (2020), Australian pyroCb smoke generates synoptic-scale stratospheric anticyclones, *Geophysical Research Letters*, *47*(13), e2020GL088,101, doi:https://doi.org/10.1029/2020GL088101.

Kablick, G., D. Allen, M. Fromm, and G. Nedoluha (December 2020), Australian pyroCb smoke generates synoptic-scale stratospheric anticyclones, *American Geophysical Union - Fall Meeting*.

Kablick, G., D. Allen, M. Fromm, and G. Nedoluha (January 2022), PyroCb Smoke-Generated SWIRLs: A Connection between Biomass Burning and Stratospheric Dynamics, *24th Conference on Atmospheric Chemistry; American Meteorological Society Annual Meeting*.

Kablick, G., D. Allen, M. Fromm, and G. Nedoluha (March 2020), A quantitative examination of large stratospheric pyroCb plumes with CALIPSO and MLS (with a shout out to CloudSat), *National Aeronautics and Space Administration - CALIPSO/ CloudSat Science Team Meeting, Boulder, CO*.

Lee, S., G. Kablick, Z. Li, C. Jung, Y. Choi, J. Um, and W. Choi (2020), Examination of effects of aerosols on a pyrocb and their dependence on fire intensity and aerosol perturbation, *Atmospheric Chemistry and Physics*, *20*(6), 3357–3371, doi:10.5194/acp-20-3357-2020.

Peterson, D., J. Campbell, E. Hyer, M. Fromm, G. Kablick, J. Cossuth, and M. DeLand (2018), Wildfire-driven thunderstorms cause a volcano-like stratospheric injection of smoke, *Clim. Atmos. Sci.*, *1*, 30.

Peterson, D., M. Fromm, R. McRae, J. Campbell, E. Hyer, G. Taha, C. Camacho, G. Kablick, C. Schmidt, and M. DeLand (2021), Australia's black summer pyrocumulonimbus super outbreak reveals potential for increasingly extreme stratospheric smoke events, *npj Climate and Atmospheric Science*, *4*(1), 1–16, doi:https://doi.org/10.1038/s41612-021-00192-9.

Pumphrey, H., M. Schwartz, M. Santee, G. Kablick, M. Fromm, and N. Livesey (2021), Microwave Limb Sounder (MLS) observations of biomass burning products in the stratosphere from Canadian forest fires in August 2017, *Atmospheric Chemistry and Physics*, *21*(22), 16,645–16,659, doi:https://doi.org/10.5194/acp-21-16645-2021.

Ricchiazzi, P., S. Yang, C. Gautier, and D. Sowle (1998), SBDART: A research and teaching software tool for plane-parallel radiative transfer in the Earth's atmosphere, *B. Am. Meteorol. Soc.*, *79*(10), 2101–2114.